Available online at www.sciencedirect.com
ScienceDirect
International Journal of Mass Spectrometry 267 (2007) 139–147
International Journal of Mass Spectrometry
www.elsevier.com/locate/ijms

Doubly protonated 1,3,5-trimethylenebenzene ($C_9H_{11}^{2+}$) and homologous $C_7H_7^{2+}$ and $C_8H_9^{2+}$ dications: Structures and unimolecular fragmentation patterns

Petr Milko [a], Jana Roithová [a,*], Detlef Schröder [a], Helmut Schwarz [b]

[a] *Institute of Organic Chemistry and Biochemistry, Academy of Sciences of the Czech Republic, Flemingovo nám. 2, 166 10 Prague, Czech Republic*
[b] *Institutfür Chemie der Technischen Universität Berlin, Strasse des 17, Juni 135, D-10623 Berlin, Germany*

Received 31 October 2006; received in revised form 31 January 2007; accepted 20 February 2007
Available online 23 February 2007

In the memory of Sharon G. Lias.

Abstract

Structures and fragmentation patterns of $C_7H_7^{2+}$, $C_8H_9^{2+}$, and $C_9H_{11}^{2+}$ dications generated from various precursors are studied by means of mass spectrometry in combination with density functional theory calculations. It is shown that double protonation of the prototype hydrocarbon triradical 1,3,5-trimethylenebenzene (C_9H_9), similar to single protonation, leads to relative stabilization of the doublet state so that it becomes the ground state of the radical dication. The preferred structures of the $C_9H_{11}^{2+}$ manifold are best described as primary, secondary, or tertiary alkyl cations attached to a benzene radical-cation core. The most abundant fragmentation corresponds to dehydrogenation. The also observed charge-separation fragmentations of the dications can be rationalized on the basis of the preferred molecular structures. In addition, a brief comparison of the dicationic systems $C_7H_7^{2+}$, $C_8H_9^{2+}$, and $C_9H_{11}^{2+}$ reveals that while the larger aromatic dications do indeed bear a structural memory, the lower homologues $C_7H_7^{2+}$ and $C_8H_9^{2+}$ completely lose the structural identity of their neutral precursors.

Keywords: Dications; DFT calculations; Mass spectrometry; Protonation; Triradicals

1. Introduction

Multiradicals, either derived from organic compounds as free species or being complexed to a metal, represent a timely, attractive topic of research [1–3]. Current investigations of multiradicals are directed toward the understanding of their chemical behavior as well as toward the description of the effects an external environment exerts on their electronic structures. In the latter context, protonation of multiradicals belongs to the more often studied effects [4–7]. As to energetic ordering of spin isomers of multiradicals derived from simple organic compounds, it has been shown that single protonation usually leads to a stabilization of the low-spin states of such molecules in that these become the ground states whereas the high-spin states represent electronically excited configurations [6,7]. Thus, a change of pH might offer a reversible switch between low- and high-spin states of a molecule in solution. This aspect constitutes a topic in its own right [8].

Here, we present an experimental and theoretical study of the structures and fragmentation patterns of $C_9H_{11}^{2+}$ dications, generated by dissociative ionization from 1,3,5-trimethylbenzene (C_9H_{12}), where the hydrogen atom is preferentially cleaved from one of the methyl groups (see below). So formed ions thus formally represent doubly protonated 1,3,5-trimethylenebenzene (TMB). The ground state of this prototype hydrocarbon triradical corresponds to a high-spin quartet state, and the first excited doublet state lies 0.54 eV above the quartet [6,9]. Recently, the effect of ionization and protonation of TMB has been studied [6]. It has been found that both ionization and protonation strongly stabilize the low-spin states. We will show that double protonation also leads to a stabilization of the low-spin state of TMB. Further, structural aspects and unimolecular reactivities of dicationic $C_9H_{11}^{2+}$ species and the related analogs $C_7H_7^{2+}$ and $C_8H_9^{2+}$ on their doublet potential-energy surfaces are studied.

* Corresponding author. Tel.: +420 2 20 183 117; fax: +420 2 20 183 583.
E-mail address: jana.roithova@uochb.cas.cz (J. Roithová).

1387-3806/$ – see front matter © 2007 Elsevier B.V. All rights reserved.
doi:10.1016/j.ijms.2007.02.027

2. Experimental and computational details

The experiments were performed with a modified VG ZAB/HF/AMD four-sector mass spectrometer of BEBE configuration (B stands for magnetic and E for electric sector), which has been described in detail previously [10]. The dications of interest were generated by 70 eV electron ionization of the corresponding neutral precursor molecules (see text) and accelerated by a potential of 8 kV. The unimolecular fragmentations of the dications of interest having 16 keV kinetic energy were monitored by recording metastable ion (MI) spectra. To this end, the ions were mass-selected by means of B(1)/E(1) and the unimolecular fragmentations of metastable ions occurring in the field-free region preceding the second magnet were recorded by scanning B(2). In order to determine the kinetic energy release (KER) associated with charge-separation fragmentations, the corresponding precursor ions were mass-selected by B(1) and fragmentations were monitored by scanning E(1). The KER was then determined from the horn-to-horn distance of the dished-top peak using established procedures [11]. The $C_xH_y^+$ dications are isobaric with ions of the type $^{13}CC_{x-1}H_{y-1}^{2+}$; and appropriate corrections have to be made. The dominant MI fragmentation of all dications studied corresponds to dehydrogenation. Even after correction for the contributions of isobaric impurities to this channel, dehydrogenation remains by far the most dominant process and exceeds charge-separation reactions by roughly three orders of magnitude. As to the latter, the interferences due to contributions of $^{13}CC_6H_6^{2+}$ and $^{13}CC_7H_8^{2+}$ dications in the MI spectra of $C_7H_7^{2+}$ and $C_8H_9^{2+}$, respectively, are negligible; therefore, these spectra are not corrected any further. For the isobaric pair of $^{13}CC_8H_{10}^{2+}$ and $C_9H_{11}^{2+}$, however, both dications contribute to the signals at *m/z* 91 and 92 in the MI spectra. The contributions of the interference signals are estimated based on measurements of the absolute ion currents of the MI spectra of $C_9H_{10}^{2+}$ with consideration of the ^{13}C natural abundance as well as the expected isotope pattern for the various fragmentations [12]. The reported ratios of H_2, HD, and D_2 losses from [2,4,6-D_3]-1,3,5-trimethylbenzene are corrected analogously. The corrected MI spectra are given in Table 1. All spectra were accumulated with the AMD-Intectra data system; 5–15 scans were averaged to improve the signal-to-noise ratio. Final data were derived from at least 3 independent measurements with an experimental error smaller than ±5%. [2,4,6-D_3]-1,3,5-Trimethylbenzene (86 at.% D) was prepared by refluxing mesitylene with an excess of D_2O (98 at.% D) in the presence of 5 mol.% CF_3COOH.

The calculations were performed using the density functional theory method B3LYP [13–15] in conjunction with 6-311G* triple-zeta basis set as implemented in the Gaussian 03 suite [16]. For all optimized structures, frequency analysis at the same level of theory was performed in order to assign them as genuine minima or transition structures on the potential-energy surface as well as to calculate zero-point vibrational energies (ZPVEs). Relative energies (E_{rel}) of the structures given below are calculated from energies at 0 K and are anchored to the doublet ground states of isomers $\mathbf{9}^{2+}$ for $C_7H_7^{2+}$, $\mathbf{15}^{2+}$ for $C_8H_9^{2+}$, and $\mathbf{1}^{2+}$ for $C_9H_{11}^{2+}$, respectively. The charge and spin density is delocalized in all structures calculated. In this context it is also stressed that all structures shown in Scheme 1 and in the Charts 1–3 should be understood as sketches with formally located charges and radical sites, rather than indication of a particular preference for one of the various mesomeric structures. For all calculated structures, the π-orbitals located on the exocyclic sp^2 carbon atoms are parallel with the π-orbitals of the five- or six-membered rings. Dications $\mathbf{4}^{2+}$, $\mathbf{5}^{2+}$, and $\mathbf{6}^{2+}$ form an exception, because their six-membered is not planar and consequently the π-orbitals of the exocyclic methylene groups are not aligned with the π-orbitals of the rings. Further details, e.g., geometries, charge and radical distributions, etc., are available upon request from the corresponding author.

3. Results and discussion

3.1. Ground-state multiplicity of doubly protonated trimethylenebenzene

The effect of double protonation on the electronic structure of trimethylenebenzene is explored by density functional theory (DFT) calculations. For a quantitative examination of the doublet-quartet energy-splitting in the system, multireference computational techniques are indicated, and DFT methods can obviously only provide qualitative insight to the problem. To estimate the limitations of the B3LYP method, the neutral system is considered first, and the results are compared with previous

Table 1
Relative abundances[a,b] of charge-separation fragments of $C_9H_{11}^{2+}$ generated from different precursors

	Precursor of $C_9H_{11}^{2+}$				
	1,3,5-Trimethylbenzene	1,2,4-Trimethylbenzene	*para*-Ethylmethylbenzene	*n*-Propylbenzene	*iso*-Propylbenzene
$C_8H_8^+ + CH_3^+$	12	4	2	0	1
$C_7H_x^+ + C_2H_{(11-x)}^{+b}$	75	87	86	83	88
$C_7H_8^+ + C_2H_3^{+b}$	27	33	33	3	18
$C_7H_7^+ + + C_2H_4^{+b}$	48	54	53	80	70
$C_6H_6^+ + C_3H_5^+$	13	9	12	17	11

[a] The abundances are determined by integration of the area of the dished-top peak corresponding to the heavier fragment.

[b] The composite signals corresponding to the $C_7H_7^+$ and $C_7H_8^+$ ions were integrated together and corrected for the intensity of $C_7H_7^+$ and $^{13}CC_6H_7^+$ ions originating from fragmentation of $^{13}CC_8H_{10}^{2+}$. The relative ratios of $C_7H_7^+$ and $C_7H_8^+$ signals were determined from heights of the outer horns of the composite peak. The heights of the signals were again corrected for the contributions due to fragmentations of $^{13}CC_8H_{10}^{2+}$.

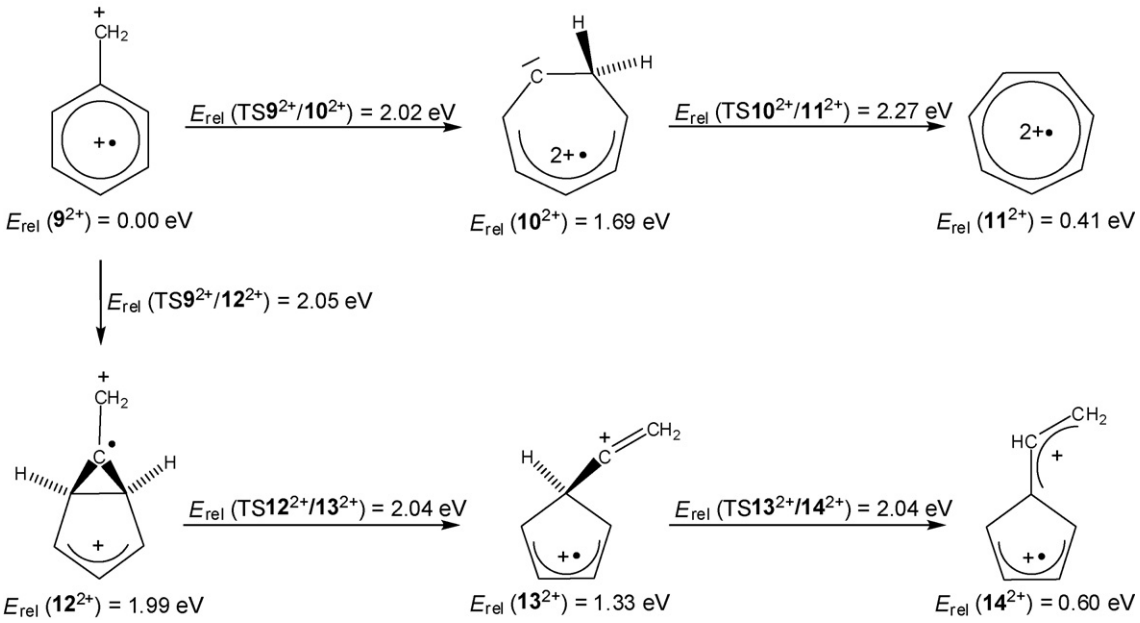

Scheme 1. Reaction pathways leading to a ring expansion or contraction of the dication $C_7H_7^{2+}$ with a structure derived from a benzylium ion ($\mathbf{9}^{2+}$). Energies are given relative to $E_{rel}(\mathbf{9}^{2+}) = 0.00$ eV. The total energy at 0 K of the doublet ground state of $\mathbf{9}^{2+}$ amounts to −270.060982 Hartree.

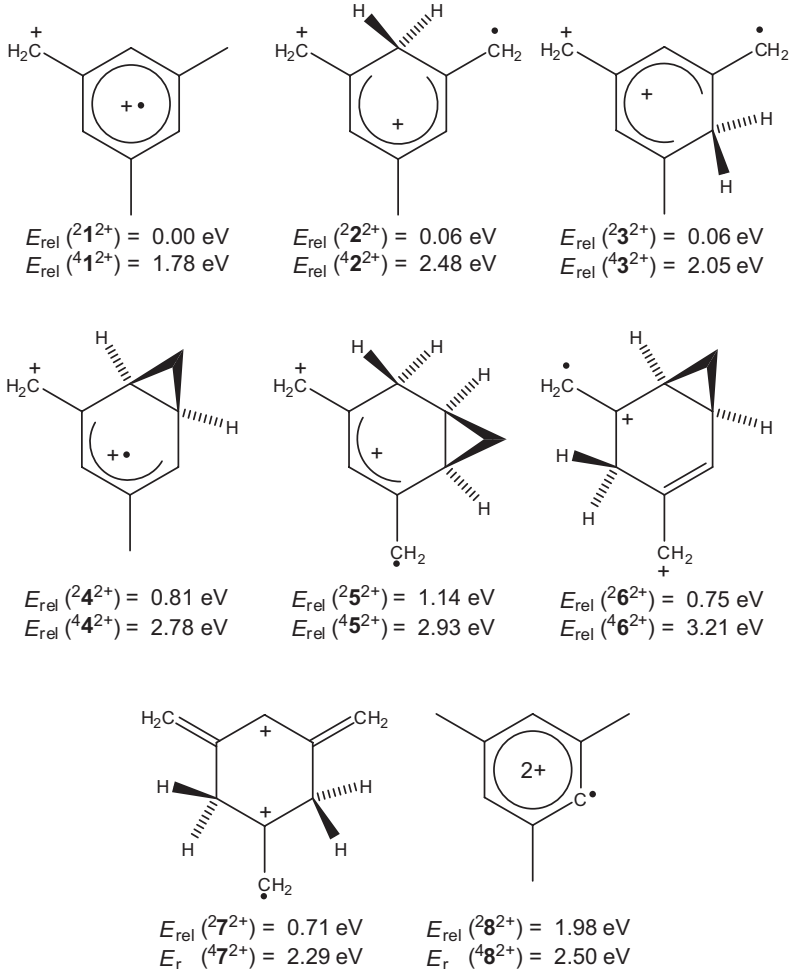

Chart 1. Selected isomers of $C_9H_{11}^{2+}$ dications obtained upon double protonation of 1,3,5-trimethylenebenzene. The total energy of the doublet ground state $\mathbf{1}^{2+}$ at 0 K ($E_{rel} = 0.00$ eV) amounts to −348.708177 Hartree.

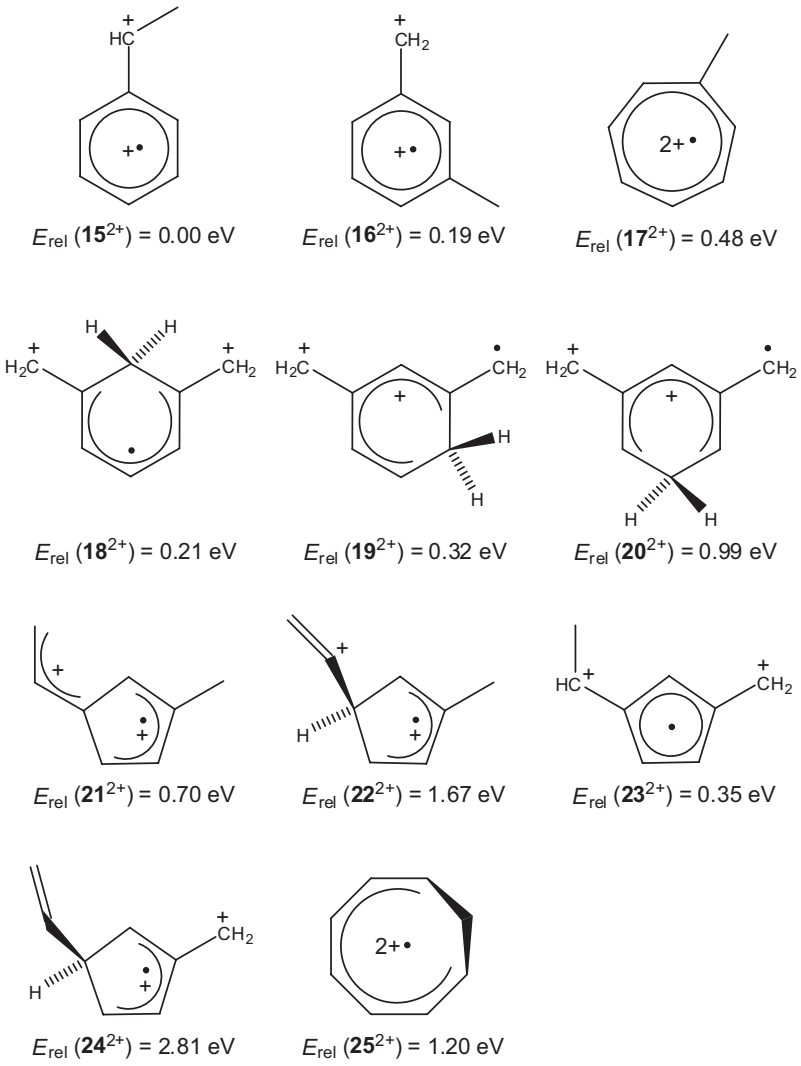

Chart 2. Selected isomers of $C_8H_9^{2+}$ dications; only doublet states of the dications were considered. The total energy of the doublet ground state of **15**$^{2+}$ at 0 K (E_{rel} = 0.00 eV) amounts to −309.396034 Hartree.

findings obtained in high-level multireference calculations [6]. Thus, the B3LYP/6-311G* method correctly predicts a quartet ground state of neutral TMB. The closest doublet state lies 0.44 eV higher in energy than the quartet. In comparison, the energy splitting calculated using CASPT2 amounts to 0.54 eV [6]. Accordingly, while the B3LYP method may slightly underestimate the energy difference between the two states, it serves as a computationally much less demanding method to get useful insight into the electronic situations of this type of multiradicals [17,18].

Protonation of trimethylenebenzene can take place either at a carbon atom of the ring or at one of the methylene groups. Protonation at the methylene group is much more favored [6]. Further, it has been shown that in both cases the low-spin state of protonated TMB is substantially more stable than the high-spin state [6]. Our B3LYP calculations predict the doublet state of methylene-protonated TMB as 1.51 eV more stable than the quartet state; this agrees reasonably well with the splitting of 1.60 eV predicted by the CASPT2 method [6]. Double protonation of TMB taking place at two methylene groups (dication **1**$^{2+}$, Chart 1) also leads to a stabilization of the low-spin state: the ground state corresponds to a doublet, whereas the quartet is 1.78 eV higher in energy. Besides protonation at the methylene groups of TMB, also protonation at the ring carbon atoms is feasible. Similar to single protonation, these protonated isomers are higher in energy, although the energy differences are quite small for the doublet ground states (Chart 1). Thus, while the first protonation takes almost exclusively place at a methylene group, the second proton can be attached to either another methylene group or in the *ortho*- or *para*-positions of the ring with respect to the methyl group formed by the first protonation. Other isomers are also conceivable, but an exploratory survey indicates that they lie much higher in energy. Note that protonation at the *ipso*-position relative to the methylene group is associated with cyclization to the structures **4**$^{2+}$, **5**$^{2+}$, and **6**$^{2+}$. Further, the doublet states of all isomers are by far energetically preferred over quartet states. Accordingly, double protonation has a similar effect on electronic structure as single protonation.

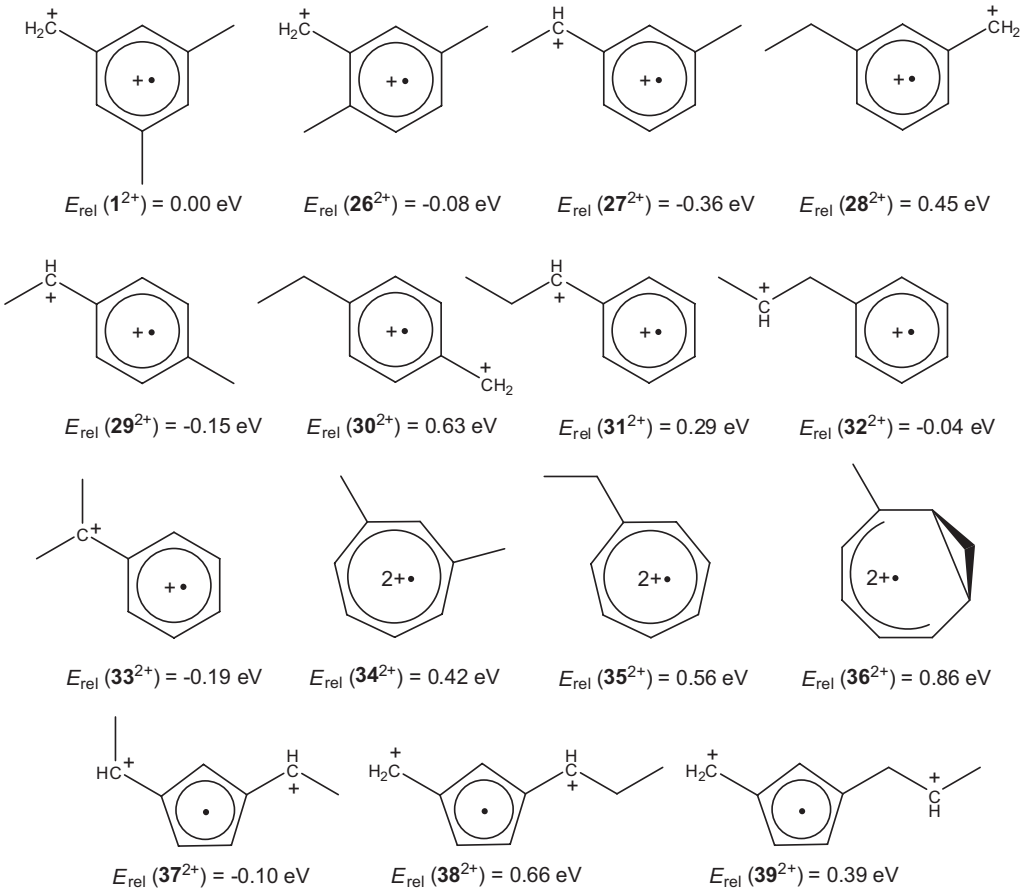

Chart 3. Selected isomers of $C_9H_{11}{}^{2+}$ dications; only doublet states of the dications were considered. The total energy of the doublet ground state of $\mathbf{1}^{2+}$ at 0 K (E_{rel} = 0.00 eV) amounts to −348.708177 Hartree.

3.2. Fragmentations of doubly protonated trimethylenebenzene

Being a dication, doubly protonated trimethylenebenzene (or its isomers) can be generated by dissociative ionization of 1,3,5-trimethylbenzene (C_9H_{12}). In the following, only the more stable doublet states of the dications are considered, and it is further assumed that the hydrogen atom in the neutral C_9H_{12} precursor upon dissociative double ionization is eliminated from one of the methyl groups, because the $C_9H_{11}{}^{2+}$ isomer generated via elimination of a hydrogen atom from a ring position (i.e., $^2\mathbf{8}^{2+}$) is 1.98 eV higher in energy than $^2\mathbf{1}^{2+}$ (see Chart 1).

Fig. 1a shows the metastable ion spectrum of $C_9H_{11}{}^{2+}$ generated from 1,3,5-trimethylbenzene. The most abundant unimolecular fragmentation of the dication corresponds to the loss of molecular hydrogen. This fragmentation route appears as a rather general process for organic dications [19–24]. Dehydrogenation is the only unimolecular decomposition pathway of doubly protonated TMB in which the two charges remain also in the hydrocarbon fragment. For organic dications with lower ratios of hydrogen to carbon atoms, often also losses of atomic hydrogen are observed [23,24]. The remaining fragmentations are much less abundant (by a factor of 10^3) and correspond to charge separation of the parent dication in which two singly charged ions are formed. The large amount of energy being released as kinetic energy (KER) is reflected in the dished-top shapes of the peaks [25] and can be estimated from the horn-to-horn distances [11]. The most abundant charge separation of $C_9H_{11}{}^{2+}$ corresponds to the loss of $C_2H_4{}^+$ (KER = 3.06 eV), followed by expulsion of another C_2-fragment $C_2H_3{}^+$(KER = 2.57 eV). Two minor charge-separation channels are associated with the formation a methyl cation (KER = 2.51 eV) and of $C_3H_5{}^+$ (KER = 3.48 eV). The kinetic energy released is associated with the height of the reverse energy barrier for the given fragmentation and is often characteristic of ion structures [11].

In order to further elucidate the fragmentation mechanism, the $C_9H_8D_3{}^{2+}$ dication generated by dissociative double ionization of [2,4,6-D_3]-1,3,5-trimethylbenzene is considered. Molecular hydrogen is eliminated from the $C_9H_8D_3{}^{2+}$ dication as H_2, HD, and D_2 in a 80:19:1 ratio, where the sum is normalized to 100; the data are corrected for the contribution from $^{13}C^{12}C_8H_7D_3{}^{2+}$, and the experimental error is ±1. If complete equilibration of all hydrogen/deuterium atoms of $C_9H_8D_3{}^{2+}$ prior to dissociation is assumed, a ratio of H_2:HD:D_2 = 50.9:43.6:5.5 is expected. However, as elimination of deuterium is usually associated with a kinetic isotope effect (KIE), consideration of a corresponding KIE of 3.3 per deuterium atom leads to a calculated ratio of H_2:HD:D_2 = 79:20:1; this is perfectly consistent with the experimental findings. This

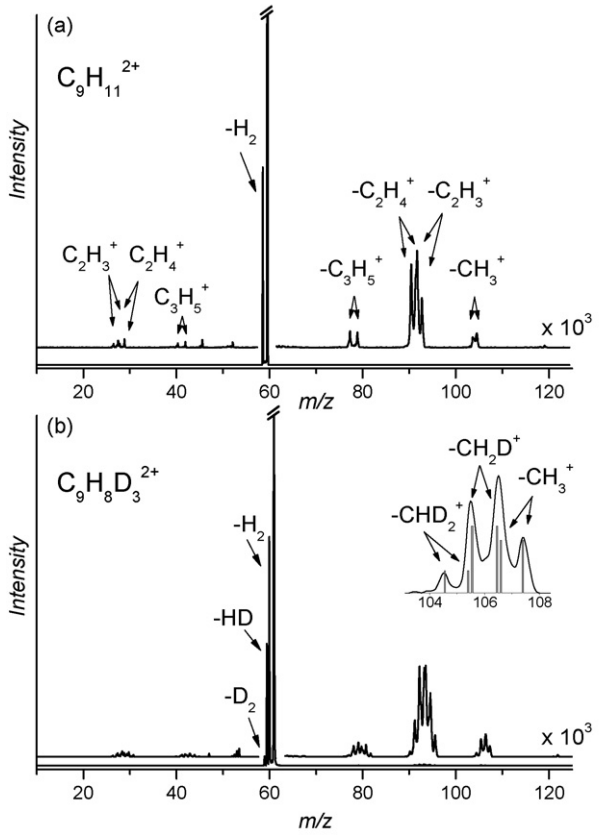

Fig. 1. Metastable ion spectra of (a) $C_9H_{11}^{2+}$ generated from 1,3,5-trimethylbenzene and (b) $C_9H_8D_3^{2+}$ generated from [2,4,6-D_3]-1,3,5-trimethylbenzene; the parent-ion signals are off-scale. The inset shows an approximate deconvolution of the composite peak corresponding to the losses of methyl cations $CH_{3-x}D_x^+$ (x = 0–2) from $C_9H_8D_3^{2+}$. Note that the spectra shown are not corrected for the contributions of $^{13}CCH_3^+$ and $C_2H_3^+$ eliminations from isobaric $^{13}CC_8H_{10}^{2+}$ (see Section 2); the corrected intensities are given in Table 1.

result suggests that all hydrogen and deuterium atoms of the $C_9H_8D_3^{2+}$ dication are completely equilibrated prior to the dehydrogenation step [26,27]. In principle, a certain combination of specific mechanisms for dehydrogenation of $C_9H_8D_3^{2+}$ could also lead to the same ratio of H_2, HD, and D_2 eliminations; however, this scenario is considered less probable and therefore not pursued any further. We note that the equilibration of the H/D atoms can also take place already in the stage of the parent dication $C_9H_9D_3^{2+}$, that is before the elimination of an H atom from one of the methyl groups. This question could be resolved by an analysis of the ratio of H and D losses from the $C_9H_9D_3^{2+}$ dication, which, however, is prevented in the experiment due to the fact that elimination of molecular hydrogen is more pronounced than that of atomic hydrogen and D and H_2 eliminations lead to dications of the same nominal mass.

Similar to dehydrogenation, scrambling of the hydrogen/deuterium atoms prior to methyl cation expulsion is also indicated by the experimental data. The inset in Fig. 1b shows the decomposition of the signal corresponding to the loss of a methyl cation to its separate components corresponding to CH_3^+, CH_2D^+, and CHD_2^+. The ratio of the labeled fragments is determined as 37:47:16, respectively (the sum is normalized to 100, the estimated error is ±4). If complete scrambling of all hydrogen/deuterium atoms is assumed, then a ratio of CH_3^+:CH_2D^+:CHD_2^+ = 34:51:15 is expected in good agreement with experiment. As less than 1% is predicted for the expulsion of CD_3^+, this process cannot clearly be discerned in Fig. 1b. Likewise, the eliminations of other charged fragments are associated with complex labeling patterns which in part also overlap with each other such that no further quantitative analysis is pursued. For the same reason, also no further attempts for additional, specific isotope labeling experiments were undertaken, because the regiospecific information often derived from selective labeling is lost in the present system. By analogy with the dehydrogenation and the elimination of a methyl cation, it is expected that also other fragmentations occur only after or concurrently with complete scrambling of the H/D atoms.

Instead, the mechanisms for the eliminations of charged fragments are analyzed on the basis of a comparison with fragmentations of other, structurally related radical dications and complemented by density functional theory calculations. Note that the attempt to derive fragmentation mechanisms for small and medium-sized dications on the basis of comparison with the corresponding monocationic species is of limited significance. At first, the high positive charge experienced by dications often leads to "non-clasical" structures [28]. The case of the benzene dication may serve as a suitable example: Instead of the expected structure with a six-membered ring, the global minimum corresponds to a pyramidal structure with a five-membered C_5H_5 base and CH group at the apex [29]. For a review on "pyramidal cations" see: ref. [30]. Further, fragmentations of organic dications are by far dominated by eliminations of atomic and mainly molecular hydrogen. Eliminations of larger fragments are usually associated with charge separation and therefore fundamentally differ from those observed for singly charged ions. Thus, an independent exploration of the dication surfaces is required.

First, the fragmentations of $C_7H_7^{2+}$ generated from toluene as well as cycloheptatriene are probed. Metastable ions generated from these two molecules yield identical spectra (Fig. 2a), which suggests that prior to the fragmentation of $C_7H_7^{2+}$ also structural reorganization has taken place. The most abundant charge-separation process corresponds to the expulsion of a $C_3H_3^+$ monocation, and two other pathways lead to the losses of $C_2H_4^+$ and $C_2H_2^+$, respectively.

Some structures accessible by expansion or contraction of the six-membered ring of $C_7H_7^{2+}$ are displayed in Scheme 1. The most stable structure computationally found corresponds to the doublet dication radical $\mathbf{9}^{2+}$ derived from the benzylium ion (energies of all calculated $C_7H_7^{2+}$ structures are relative to $E_{rel}(\mathbf{9}^{2+})$ = 0.00 eV). The expansion to a seven-membered ring requires an activation energy of $E_{rel}(TS\mathbf{9}^{2+}/\mathbf{10}^{2+})$ = 2.02 eV. The dication $\mathbf{10}^{2+}$ lies considerably higher in energy ($E_{rel}(\mathbf{10}^{2+})$ = 1.69 eV). However, migration of a hydrogen atom via the barrier $TS\mathbf{10}^{2+}/\mathbf{11}^{2+}$ (E_{rel} = 2.27 eV) leads to the tropylium-like dication $\mathbf{11}^{2+}$ lying only 0.41 eV above $\mathbf{9}^{2+}$. The contraction of the six-membered ring via the barrier $TS\mathbf{9}^{2+}/\mathbf{12}^{2+}$ (E_{rel} = 2.05 eV) is first associated with

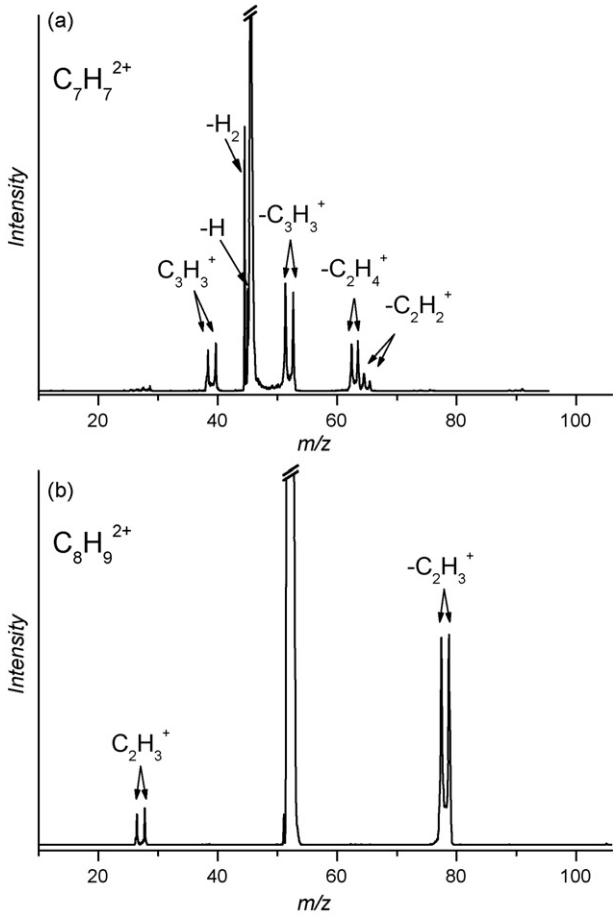

Fig. 2. Metastable ion spectra of (a) $C_7H_7^{2+}$ generated from toluene and (b) $C_8H_9^{2+}$ generated from *meta*-xylene. Note that the parent-ion signals are off-scale.

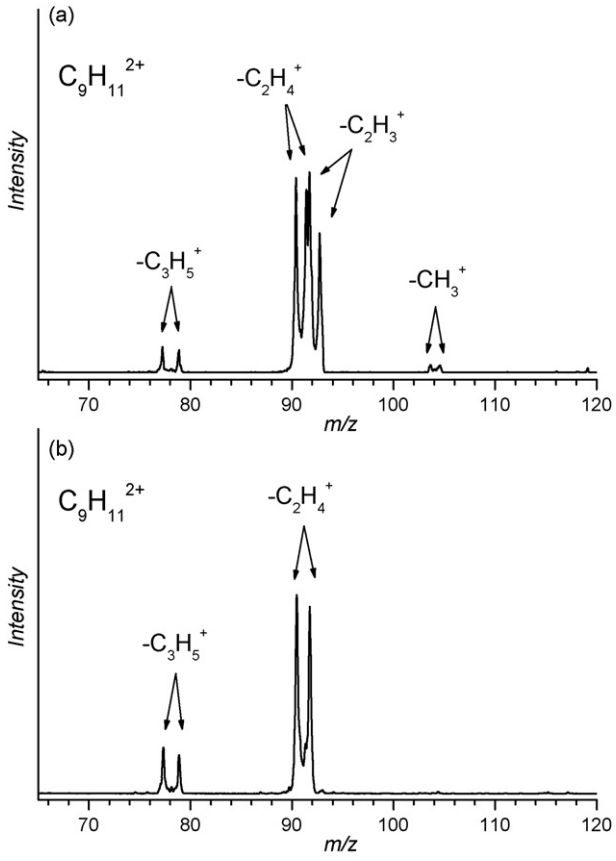

Fig. 3. Metastable ion spectra of (a) $C_9H_{11}^{2+}$ generated from 1,2,4-trimethylbenzene and (b) *n*-propylbenzene. For the sake of clarity, only fragment ions with $m/z > 65$ are shown.

the formation of a dication with a bicyclic structure $\mathbf{12}^{2+}$ ($E_{rel}(\mathbf{12}^{2+}) = 1.99$ eV). The three-membered ring is then opened ($E_{rel}(TS\mathbf{12}^{2+}/\mathbf{13}^{2+}) = 2.04$ eV) and a more stable dication $\mathbf{13}^{2+}$ ($E_{rel} = 1.33$ eV) is formed. Finally, an even more stable dication $\mathbf{14}^{2+}$ ($E_{rel} = 0.60$) is achievable via a hydrogen shift ($E_{rel}(TS\mathbf{13}^{2+}/\mathbf{14}^{2+}) = 2.04$ eV). Thus, the rearrangement from $\mathbf{9}^{2+}$ to $\mathbf{14}^{2+}$ proceeds via three almost identical energy barriers. Also in comparison, the energy barriers for both mechanisms, ring contraction and expansion, are comparable, and it is therefore expected that a variety of structures can be explored by the system before the dication $C_7H_7^{2+}$ undergoes fragmentation provided that the energy barriers for the fragmentations are higher. This condition seems to hold true at least for the charge-separation reactions of these and similar hydrocarbon dications. It has been shown in several studies of hydrocarbon dications (e.g., $C_6H_8^{2+}$ or $C_7H_8^{2+}$), where experimental and theoretical results have been combined, that the energy barriers for the dominant or even exclusive fragmentation channel, i.e., loss of H_2, are in a range of 2–3 eV [22,24,31]. As charge-separation reactions are hardly observed for these dications, their energy barriers are much higher in energy and thus certainly above the barriers for structural rearrangements. This conclusion is in agreement with the experimental observation that $C_7H_7^{2+}$ dications generated from different precursors yield identical spectra.

Next, $C_8H_9^{2+}$ dications generated from ethylbenzene, cyclooctatriene, and the three isomeric xylenes (*ortho*-, *meta*-, and *para*-dimethylbenzene) are considered. Similar to $C_7H_7^{2+}$, all $C_8H_9^{2+}$ dications generated from these precursors yield identical metastable-ion spectra (Fig. 2b). Accordingly, it can again be assumed that the ions explore a variety of isomeric structures before they undergo fragmentation. Some of the more likely isomers are displayed in Chart 2. The charge separation of $C_8H_9^{2+}$ leads almost exclusively to the pair of $C_2H_3^+$ and $C_6H_6^+$ cations. The structure of the cationic $C_6H_6^+$ species most likely corresponds to the benzene cation [32]; this assignment would also agree with the fact that the most stable structure of $C_8H_9^{2+}$ found, i.e., $\mathbf{15}^{2+}$, is derived from ethylbenzene; the energies of all structure optimized for $C_8H_9^{2+}$ dication are accordingly related to $E_{rel}(\mathbf{15}^{2+}) = 0.00$ eV. Given the experimentally evident loss of structural identity on the $C_8H_9^{2+}$ surface, we have restricted the further theoretical investigations to the most obvious structures, however.

Finally, some isomers of doubly protonated trimethylenebenzene, $C_9H_{11}^{2+}$, generated by dissociative double ionization of 1,2,4-trimethylbenzene (Fig. 3a), *para*-ethylmethylbenzene, *n*-propylbenzene (Fig. 3b), and *iso*-propylbenzene are considered. Although, the fragmentations of metastable ions generated from

all precursors are again quite similar, they are not identical (Table 1). The most apparent difference is found in the spectra of the dication generated from *n*-propylbenzene. In comparison with the spectrum obtained for $C_9H_{11}^{2+}$ generated from 1,3,5-trimethylbenzene (Fig. 1a), this spectrum does not contain a signal corresponding to the elimination of CH_3^+ and the abundance of $C_2H_3^+$ loss is almost negligible. Instead, charge separations to the pairs $C_7H_7^+ + C_2H_4^+$ and $C_6H_6^+ + C_3H_5^+$, respectively, are preferred. This result suggests that the $C_9H_{11}^{2+}$ dication derived from *n*-propylbenzene has a structure, which is more prone for charge separation leading to the most stable singly charged fragments like the benzene cation or the benzylium/tropylium ions. The hypothesis that the $C_2H_4^+$ fragment is lost from the end of *n*-propyl-chain is further tested with an experiment in which the $C_9H_{11}^{2+}$ cation is generated from *iso*-propylbenzene. In agreement, the abundance of the $C_2H_4^+$ loss is significantly lower and a substantial amount of a competing $C_2H_3^+$ elimination is observed (Table 1). The $C_9H_{11}^{2+}$ dications generated from 1,2,4-trimethylbenzene and *para*-ethylmethylbenzene show fragmentation patterns quite similar to that of the $C_9H_{11}^{2+}$ dication generated from 1,3,5-trimethylbenzene. Metastable dications generated from isomeric trimethylbenzenes lose a methyl cation in substantially higher abundance than the dications generated from the other precursors, suggesting that loss of a methyl cation is favored for the structures with a methyl group attached to the benzene ring. We note in passing that the KER measured for a particular fragmentation of $C_9H_{11}^{2+}$ ions (e.g., loss of CH_3^+) generated from different precursors are identical within the experimental error. It means that fragmentations most probably proceed with analogous mechanisms from preferred structures of $C_9H_{11}^{2+}$ dications as mentioned above. In summary, these findings suggest that the $C_9H_{11}^{2+}$ dications retain to a certain degree the structures of their neutral C_9H_{12} precursors in their formation as well as prior to their fragmentation. This finding is quite remarkable in that complete loss of structural identity has been assumed before for aromatic $C_xH_y^{2+}$ dications [19] and also many monocationic arenes show extensive H as well as C-scrambling [27].

Exploratory calculations (Chart 3) show that many structures of $C_9H_{11}^{2+}$ dications, which have only small differences in their relative energies, can actually be found. The optimized structures were selected with regard to the precursors for $C_9H_{11}^{2+}$ dications used in the experiments. While many other isomers can be considered as well, they are expected to lie higher in energy than the optimized dications and further calculations would thus not bring qualitatively new insights to the topic under study. The dication $\mathbf{27}^{2+}$ with a structure derived from *meta*-ethylmethylbenzene is found as the most stable one (the energies of all structures optimized for $C_9H_{11}^{2+}$ dication are relative to $E_{rel}(\mathbf{1}^{2+}) = 0.00\,eV$).

In a more general perspective of structural organic chemistry, a notable conclusion is that for all radical dications studied in this work, the energetically preferred structures found computationally contain six-membered rings. This finding can be rationalized on the basis of a more efficient charge separation between a six-membered ring, which formally corresponds to the benzene radical cation, and an alkyl chain, which formally bears a primary, secondary, or tertiary alkyl cation, respectively. These structures then, quite likely, also determine to some extent the course of the charge separation of the dications, namely: (i) dications comprising a methyl-substituted benzene core (e.g., $\mathbf{1}^{2+}$, $\mathbf{26}^{2+}$, $\mathbf{29}^{2+}$) yield a somewhat more pronounced methyl-cation loss, (ii) metastable ions with a structure derived from ethylbenzene ionized at the ethyl group (e.g., $\mathbf{15}^{2+}$, $\mathbf{27}^{2+}$, $\mathbf{29}^{2+}$) preferably lead to $C_2H_3^+$ loss, and (iii) dications bearing an ionized *n*-propyl group attached to the core (e.g., $\mathbf{31}^{2+}$ or $\mathbf{32}^{2+}$) preferably undergo expulsion of $C_2H_4^+$ and $C_3H_5^{2+}$ cations.

4. Conclusions

Promising perspectives for future research evolve from the fact that the often vast and rather complex fragmentation patterns of aromatic dications seem to exhibit a direct relationship to the underlying ion structures when the size of the molecules is appropriately large. Thus, whereas the dications $C_7H_7^{2+}$ as well as $C_8H_9^{2+}$ obviously have lost all structural relationship to the neutral compounds used in the ion generation, the $C_9H_{11}^{2+}$ system shows notable differences depending on the different neutral precursors used. Moreover, combination with the theoretical studies provides some chemical insight into the most favored structures of the various species in that the preferred structures of the studied organic radical dications correspond to sidechains with primary or secondary (for higher hydrocarbons also tertiary) alkyl cations with a benzene radical cation acting as a core. These structures are then reflected in the charge separation of the corresponding hydrocarbon dications. However, the most abundant fragmentation of doubly protonated trimethylenebenzene corresponds to dehydrogenation, thus yielding a dicationic fragment again, rather than a pair of singly charged products, thereby underlining the notion that dication reactivity is not at all necessarily associated with charge separation.

With regard to the effect of protonation on the state splitting of multiradicals, the computational data imply that double protonation strongly stabilizes low-spin state of trimethylenebenzene, just like single protonation does. Protonation at the methylene groups is slightly preferred.

Acknowledgements

The work was gratefully supported by the Grant Agency of the Academy of Sciences of the Czech Republic (No. KJB4040302), the Deutsche Forschungsgemeinschaft, and the Fonds der Chemischen Industrie.

References

[1] L.V. Slipchenko, T.E. Munsch, P.G. Wenthold, A.I. Krylov, Angew. Chem. Int. Ed. 43 (2004) 742.
[2] A.I. Krylov, J. Phys. Chem. A 109 (2005) 19638.
[3] J.S. Miller, Inorg. Chem. 39 (2000) 4392.
[4] J. Hoffner, M.J. Schottelius, D. Feichtinger, P. Chen, J. Am. Chem. Soc. 120 (1998) 376.
[5] Y.I. Glazechev, V.V. Khramtsov, T.A. Berezina, L.B. Volodarsky, Appl. Magn. Res. 15 (1998) 407.
[6] H.M.T. Nguyen, T.T. Hue, N.T. Nguyen, Chem. Phys. Lett. 411 (2005) 450.

[7] H.M.T. Nguyen, A. Dutta, K. Morokuma, N.T. Nguyen, J. Chem. Phys. 122 (2005) 154308.
[8] A. Dei, B. Gatteschi, C. Sangregorio, L. Sorace, Acc. Chem. Res. 37 (2004) 827.
[9] L.A. Hammad, P.G. Wenthold, J. Am. Chem. Soc. 123 (2001) 12311.
[10] C.A. Schalley, D. Schröder, H. Schwarz, Int. J. Mass Spectrom. Ion Process. 153 (1996) 173.
[11] R.G. Cooks, J.M. Beynon, R.M. Caprioli, G.R. Lester, Metastable Ions, Elsevier, Amsterdam, 1973.
[12] J. Loos, D. Schröder, W. Zummack, H. Schwarz, R. Thissen, O. Dutuit, Int. J. Mass Spectrom. 214 (2002) 105.
[13] S.H. Vosko, L. Wilk, M. Nusair, Can. J. Phys. 58 (1980) 1200.
[14] C. Lee, W. Yang, R.G. Parr, Phys. Rev. B 37 (1988) 785.
[15] B. Miehlich, A. Savin, H. Stoll, H. Preuss, Chem. Phys. Lett. 157 (1989) 200.
[16] M.J. Frisch, G.W. Trucks, H.B. Schlegel, G.E. Scuseria, M.A. Robb, J.R. Cheeseman, J.A. Montgomery Jr., T. Vreven, K.N. Kudin, J.C. Burant, J.M. Millam, S.S. Iyengar, J. Tomasi, V. Barone, B. Mennucci, M. Cossi, G. Scalmani, N. Rega, G.A. Petersson, H. Nakatsuji, M. Hada, M. Ehara, K. Toyota, R. Fukuda, J. Hasegawa, M. Ishida, T. Nakajima, Y. Honda, O. Kitao, H. Nakai, M. Klene, X. Li, J.E. Knox, H.P. Hratchian, J.B. Cross, C. Adamo, J. Jaramillo, R. Gomperts, R.E. Stratmann, O. Yazyev, A.J. Austin, R. Cammi, C. Pomelli, J.W. Ochterski, P.Y. Ayala, K. Morokuma, G.A. Voth, P. Salvador, J.J. Dannenberg, V.G. Zakrzewski, S. Dapprich, A.D. Daniels, M.C. Strain, O. Farkas, D.K. Malick, A.D. Rabuck, K. Raghavachari, J.B. Foresman, J.V. Ortiz, Q. Cui, A.G. Baboul, S. Clifford, J. Cioslowski, B.B. Stefanov, G. Liu, A. Liashenko, P. Piskorz, I. Komaromi, R.L. Martin, D.J. Fox, T. Keith, M.A. Al-Laham, C.Y. Peng, A. Nanayakkara, M. Challacombe, P.M.W. Gill, B. Johnson, W. Chen, M.W. Wong, C. Gonzalez, J.A. S Pople, Gaussian 03, Revision C.02, Gaussian, Inc., Wallingford, CT, 2004.
[17] J. Roithová, D. Schröder, H. Schwarz, Chem. Eur. J. 11 (2005) 628.
[18] J. Roithová, D. Schröder, H. Schwarz, Angew. Chem. Int. Ed. 44 (2005) 3092.
[19] P.G. Sim, W.D. Jamieson, R.K. Boyd, Org. Mass Spectrom. 24 (1989) 327.
[20] H. Perreault, L. Ramaley, F.M. Benoit, P.G. Sim, R.K. Boyd, J. Phys. Chem. A 95 (1991) 4989.
[21] S. Leach, J.H.D. Eland, S.D. Price, J. Phys. Chem. 93 (1989) 7583.
[22] J. Roithová, D. Schröder, P. Gruene, T. Weiske, H. Schwarz, J. Phys. Chem. A 110 (2006) 2970.
[23] J. Roithová, D. Schröder, J. Am. Chem. Soc. 128 (2006) 4208.
[24] J. Roithová, J. Žabka, D. Ascenzi, P. Francezschi, C.L. Ricketts, D. Schröder, Chem. Phys. Lett. 423 (2006) 254.
[25] J. Roithová, D. Schröder, H. Schwarz, J. Phys. Chem. A 108 (2004) 5060.
[26] H. Schwarz, H. Top. Curr. Chem. 73 (1978) 231.
[27] D. Kuck, Int. J. Mass Spectrom. 213 (2002) 101.
[28] K. Lammertsma, P.v.R. Schleyer, H. Schwarz, Angew. Chem. Int. Ed. Engl. 28 (1989) 1321.
[29] K. Krogh-Jespersen, J. Am. Chem. Soc. 113 (1991) 417.
[30] H. Schwarz, Angew. Chem. Int. Ed. Engl. 20 (1981) 991.
[31] J. Roithová, D. Schröder, R. Berger, H. Schwarz, J. Phys. Chem. A 110 (2006) 1650.
[32] D. Schröder, K. Schroeter, W. Zummack, H. Schwarz, J. Am. Soc. Mass Spectrom. 10 (1999) 878.